

Pyridinium-conjugated polynorbornenes for nanomolar ATP

Sensing using Indicator Displacement Assay and PET strategy

Ling-Xi Huang ^{a,‡}, Yue-Bo He ^{a,‡}, Jaewon Kim^b, Amit Sharma^c, Qian-Yong Cao ^{a,*}

Jong Seung Kim ^{b,*}

^a Department of Chemistry, Nanchang University, Nanchang 330031, P. R. China.

^b Department of Chemistry, Korea University, Seoul 02841, Korea.

^c CSIR-CSIO, Sector 30C, Chandigarh 160030, India.

‡ These two authors contributed equally to this work.

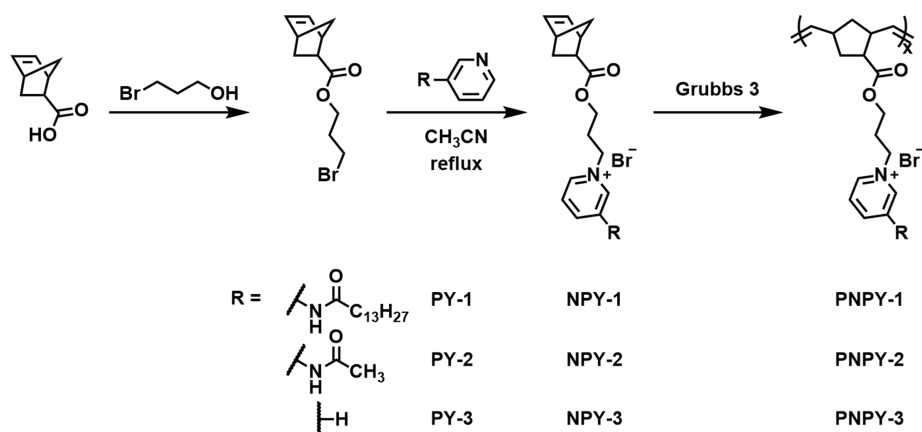
*Corresponding author. E-mail: cqyong@ncu.edu.cn (Q.-Y. Cao),

jongskim@korea.ac.kr (JSK)

Experimental Section:

Materials and Instruments:

All chemicals and reagents for the reaction are analytical pure and used without further purification. The intermediates **2**, **PY2** and **PY3** were prepared by literature method [1, 2]. A Hitachi F-4500 spectrofluorophotometer was used for fluorescence measurements. The absorption spectra were measured on a Hitachi U-3900/3900H spectrophotometer. The ¹H NMR and ¹³C NMR spectra were recorded by a Varian instrument (400 MHz). The particle size of the nanoaggregations was recorded by a Zetasizer Nano-ZS90 instrument.



Scheme S1 Synthesis route of **PNPY-n**.

General procedure for Synthesis of NPY-n:

Equal amount (1.0 mmol) of compound **4** (300 mg, 1.16 mmol) and **PY-n** ($n = 1, 2, 3$) were dissolved in acetonitrile (40 mL) under a nitrogen atmosphere. The stirred solution was heated and refluxed overnight. The solvent was evaporated in vacuo and the crude residue was purified by column chromatography ($\text{CH}_2\text{Cl}_2/\text{MeOH}$, 95: 5, v/v) to obtain **NPY-n** as a white solid.

NPY-1: Yield 70%. ^1H NMR (400 MHz, $\text{DMSO-}d_6$) δ ppm: 10.88 (s, 1H), 9.42 (s, 1H), 8.76 (d, $J = 5.7$ Hz, 1H), 8.33 (d, $J = 8.9$ Hz, 1H), 8.06 (d, $J = 2.8$ Hz, 1H), 6.11 (s, 1H), 5.82 (s, 1H), 4.73 – 4.61 (m, 2H), 4.09 (d, $J = 5.8$ Hz, 1H), 4.05 – 3.93 (m, 2H), 2.99 (s, 1H), 2.80 (s, 1H), 2.37 (d, $J = 8.3$ Hz, 2H), 2.21 (dq, $J = 12.7, 6.4$ Hz, 3H), 1.81 – 1.71 (m, 1H), 1.56 (s, 2H), 1.33 – 1.10 (m, 24H), 0.80 (d, $J = 5.7$ Hz, 3H). ^{13}C NMR (400 MHz, $\text{DMSO-}d_6$) δ ppm: 146.09, 145.40, 138.10, 132.81, 128.51, 61.35, 58.97, 49.48, 45.45, 42.88, 42.33, 30.03, 29.11. TOF-HRMS (m/z): Calcd. for ($\text{C}_{30}\text{H}_{47}\text{BrN}_2\text{O}_3$): 483.3581 ($\text{M} - \text{Br}^-$), found 483.3570 ($\text{M} - \text{Br}^-$).

NPY-2: Yield 87%. ^1H NMR (400 MHz, $\text{DMSO-}d_6$) δ ppm: 11.15 (s, 1H), 9.41 (s, 1H), 8.80 (d, $J = 6.1$ Hz, 1H), 8.43 (d, $J = 8.6$ Hz, 1H), 8.11 – 8.04 (m, 1H), 6.12 (s, 1H), 5.83 (s, 1H), 4.67 (t, $J = 7.0$ Hz, 2H), 4.00 (t, $J = 6.2$ Hz, 2H), 3.01 (s, 1H), 2.80 (s, 1H), 2.19 (t, $J = 6.6$ Hz, 2H), 2.17 – 2.11 (m, 3H), 1.77 (t, $J = 10.3$ Hz, 1H), 1.28 – 1.21 (m, 2H), 1.18 – 1.11 (m, 1H). ^{13}C NMR (400 MHz, $\text{DMSO-}d_6$) δ ppm: 170.24,

139.78, 139.57, 138.09, 134.93, 134.19, 132.81, 128.67, 61.20, 59.42, 49.51, 45.47, 42.35, 30.19, 29.12. TOF-HRMS (m/z): Calcd. for ($C_{18}H_{23}BrN_2O_3$): 314.1703 ($M - Br^- - H^+$), found 314.1712.

NPY-3: Yield 88%. 1H NMR (400 MHz, DMSO- d_6) δ ppm: 9.08 (d, $J = 6.0$ Hz, 2H), 8.60 (t, $J = 7.8$ Hz, 1H), 8.16 (t, $J = 6.9$ Hz, 2H), 6.12 (dd, $J = 5.7, 3.0$ Hz, 1H), 5.83 (dd, $J = 5.7, 2.8$ Hz, 1H), 4.66 (t, $J = 7.0$ Hz, 2H), 4.01 (t, $J = 6.0$ Hz, 2H), 2.99 (s, 1H), 2.81 (s, 1H), 2.25 (d, $J = 6.5$ Hz, 1H), 1.77 (ddd, $J = 12.4, 9.5, 3.6$ Hz, 1H), 1.27 – 1.20 (m, 2H), 1.15 (dt, $J = 11.8, 3.3$ Hz, 1H). ^{13}C NMR (400 MHz, DMSO- d_6) δ ppm: 146.09, 145.40, 138.10, 132.81, 128.51, 61.35, 58.97, 49.48, 45.45, 42.88, 42.33, 30.0, 29.11. TOF-HRMS (m/z): Calcd. for ($C_{16}H_{20}BrNO_2$): 257.1489 ($M - Br^- - H^+$), found 257.1487.

General procedure for Synthesis of PNPY-n:

Monomer **NPY-n** (0.5 mmol) and the Grubbs third-generation catalyst (1% of the amount of monomer substance) were dissolved in 5 mL of dry dichloromethane. Under nitrogen protection, the mixture was stirred at room temperature for 10 minutes, and then 1 mL of ethyl-vinyl ether was added to terminate the polymerization. It was then precipitated by crystallization in ether and concentrated to get the off-white solid **PNPY-n**.

PNPY-1: Yield 72%. 1H NMR (400 MHz, DMSO- d_6) δ ppm: 11.01 (s, 1H), 9.47 (s, 1H), 8.81 (s, 1H), 8.34 (s, 1H), 8.09 (s, 1H), 4.67 (s, 2H), 3.93 (s, 1H), 3.31 (d, $J = 2.8$ Hz, 6H), 3.08 (s, 1H), 2.76 (s, 2H), 2.19 (s, 2H), 1.82 (s, 2H), 1.53 (s, 3H), 1.16 (s, 14H), 0.78 (s, 2H). ^{13}C NMR (400 MHz, DMSO- d_6) δ ppm: 173.05, 139.55, 128.77, 36.50, 31.74, 29.51, 29.19, 29.00, 25.05, 22.54, 14.37. GPC (THF, polystyrene standards): $M_n = 33240$, $M_w = 34902$, and PDI = 1.05.

PNPY-2: Yield 70%. 1H NMR (400 MHz, DMSO- d_6) δ ppm: 11.38 (s, 1H), 9.44 (s, 1H), 8.85 (s, 1H), 8.49 (s, 1H), 8.09 (s, 1H), 4.69 (s, 2H), 4.00 (d, $J = 40.9$ Hz, 2H), 3.08 (s, 1H), 2.78 (s, 1H), 2.17 (d, $J = 21.2$ Hz, 3H), 1.87 (s, 1H), 1.50 (s, 1H), 1.20 (s,

1H). ^{13}C NMR (400 MHz, $\text{DMSO-}d_6$) δ ppm: 170.25, 139.63, 134.72, 134.11, 129.85, 128.66, 30.22, 24.27. GPC (THF, polystyrene standards): $M_n = 33199$, $M_w = 33858$, and PDI = 1.05.

PNPY-3: Yield 70%. ^1H NMR (400 MHz, $\text{DMSO-}d_6$) δ ppm: 9.13 (s, 2H), 8.62 (s, 1H), 8.17 (s, 2H), 4.69 (s, 2H), 4.06 (s, 1H), 3.93 (s, 1H), 3.11 (s, 1H), 2.78 (s, 2H), 2.24 (s, 2H), 1.84 (s, 2H), 1.49 (s, 1H), 1.15 (s, 1H). ^{13}C NMR (400 MHz, $\text{DMSO-}d_6$) δ ppm: 146.14, 145.27, 128.46, 61.07, 58.67, 30.08. GPC (THF, polystyrene standards): $M_n = 33068$, $M_w = 34721$, and PDI = 1.05.

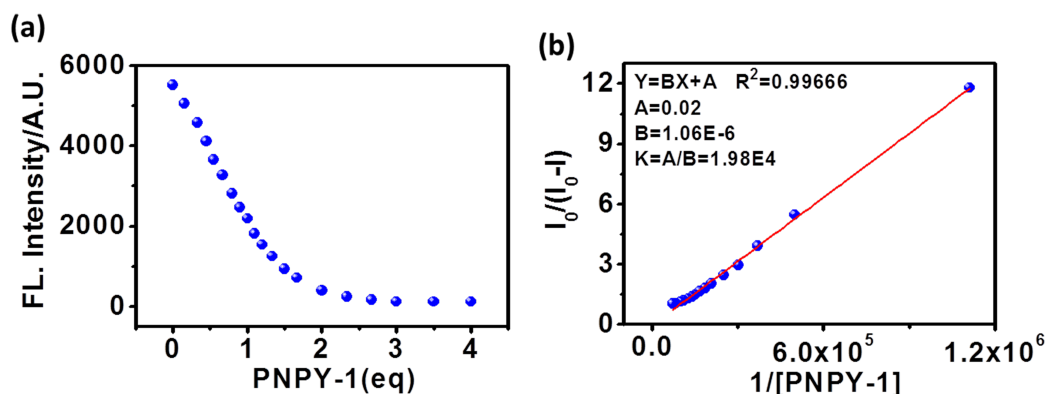


Fig. S1 (a) Fluorescence intensity of UD at 515 nm versus the number of equivalents of **PNPY-1**. (b) The binding constant of **PNPY-1/UD** using the Benesi-Hildebrand method.

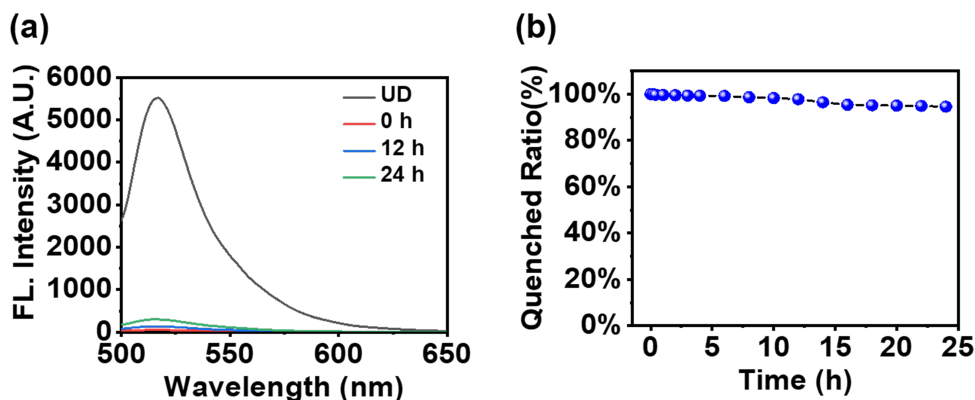


Fig. S2 (a) Fluorescence spectra and (b) relative fluorescence quenching ratios (%) of UD (6 μM , $\lambda_{\text{ex}} = 490$ nm) at 515 nm upon titration 2 equivalents of **PNPY-1** storage different time in HEPES (10 mM, pH = 7.4) buffer solution.

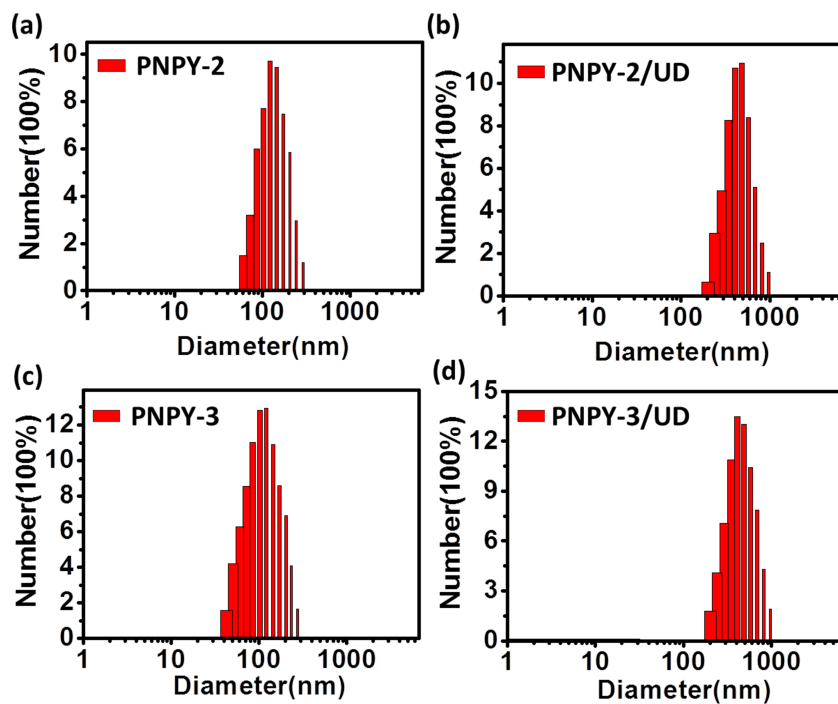


Fig. S3 The size distribution of (a) PNPY-2; (b) PNPY-2/UD; (c) PNPY-3; (d) PNPY-3/UD.

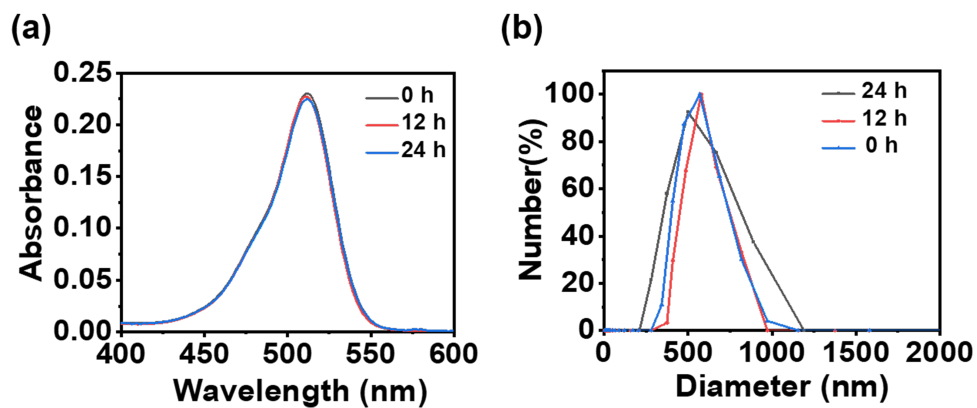


Fig. S4 (a) UV-vis spectra and (b) size distribution of PNPY-1/UD (12 μ M/6 μ M) with storage different time in a HEPES (10 mM, pH = 7.4) buffered solution.

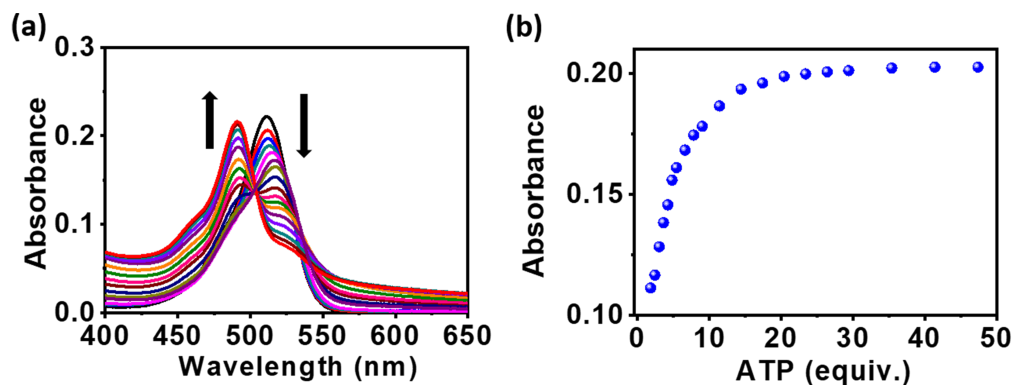


Fig. S5 (a) UV-vis spectra of **PNPY-1/UD** (12 μM/6 μM, $\lambda_{\text{ex}} = 490$ nm) upon addition of various amounts of ATP in a HEPES (10 mM, pH = 7.4) buffered solution. (b) UV titration curve of **PNPY-1/UD** at 490 nm versus the equiv. of ATP.

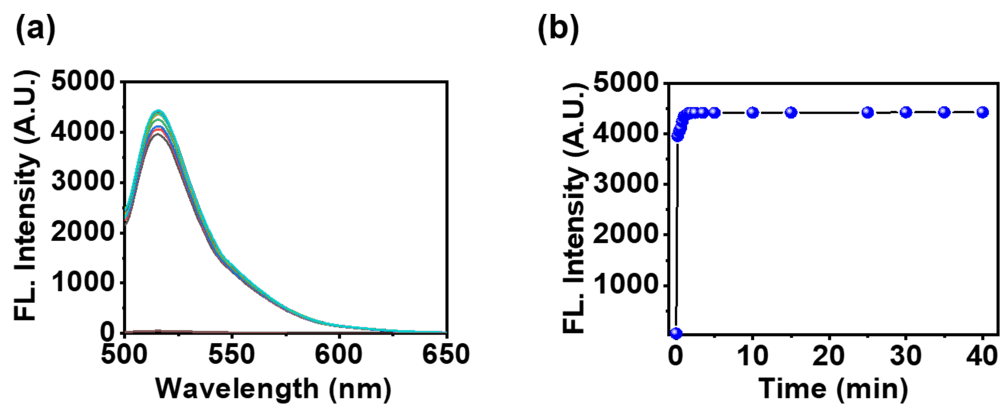


Fig. S6 The time course of fluorescence spectra of (a) **PNPY-1/UD** (6 μM, $\lambda_{\text{ex}} = 490$ nm) and the fluorescence intensity of **UD** at 515 nm (b) **PNPY-1/UD** (6 μM, $\lambda_{\text{ex}} = 490$ nm) upon addition of 20 equiv of ATP in HEPES (10 mM, pH = 7.4) buffer solution.

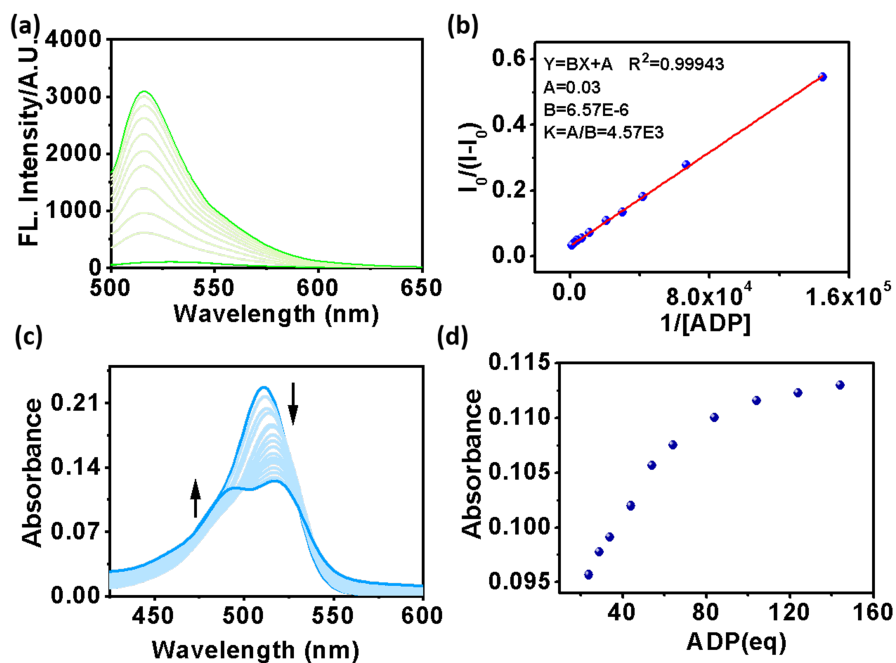


Fig. S7 The fluorescence (a) and UV-vis (c) spectra of **PNPY-1/UD** ($6 \mu\text{M}$, $\lambda_{\text{ex}} = 490 \text{ nm}$) upon addition of various amounts of ADP in HEPES (10 mM, pH = 7.4) buffer solution. The binding constant of **PNPY-1/ADP** using the Benesi-Hildebrand method (b) and UV absorbance of **PNPY-1/UD** at 490 nm (d) versus the equiv of ADP.

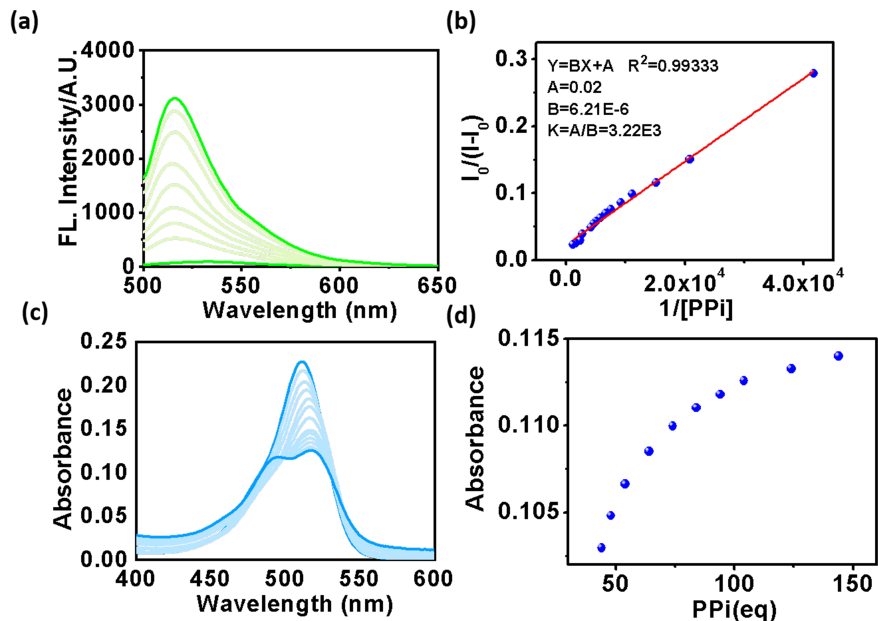


Fig. S8 The fluorescence (a) and UV-vis (c) spectra of **PNPY-1/UD** ($6 \mu\text{M}$, $\lambda_{\text{ex}} = 490 \text{ nm}$) upon addition of various amounts of PPI in HEPES (10 mM, pH = 7.4) buffer solution. The binding constant of **PNPY-1/PPI** using the Benesi-Hildebrand method (b) and UV absorbance of **PNPY-1/UD** at 490 nm (d) versus the equiv of PPI.

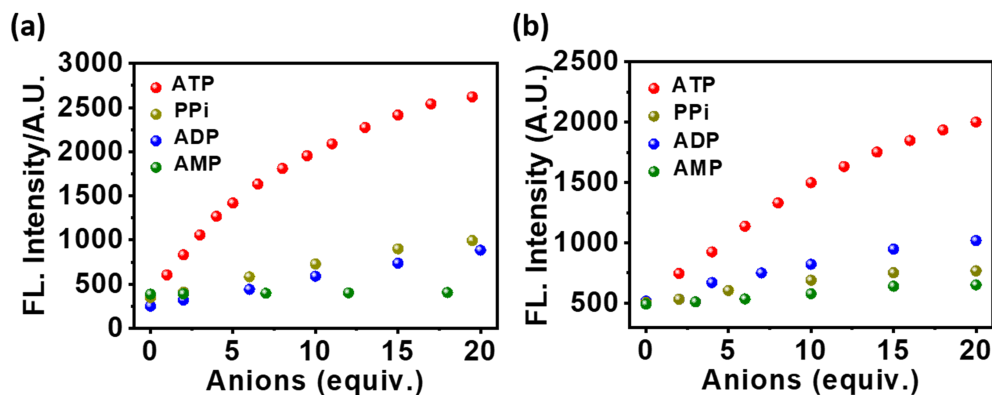


Fig. S9 Fluorescence intensity of (a) PNPY-2/UD (36 $\mu\text{M}/6 \mu\text{M}$, $\lambda_{\text{ex}} = 490 \text{ nm}$) and (b) PYNP-3/UD (120 $\mu\text{M}/6 \mu\text{M}$, $\lambda_{\text{ex}} = 490 \text{ nm}$) at 515 nm versus the equiv of anions.

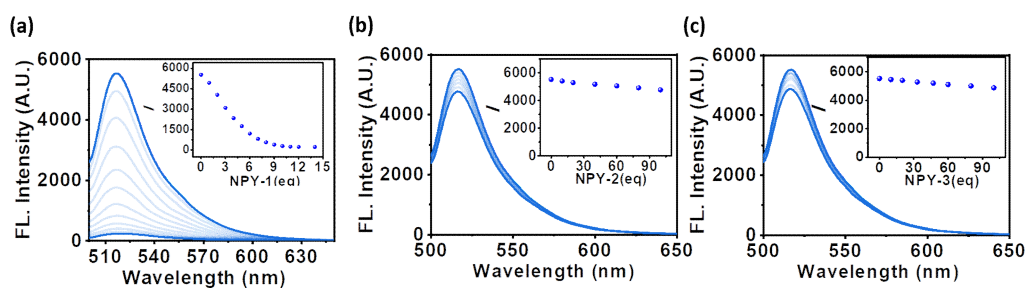


Fig. S10 Fluorescence spectra of UD (6 μM , $\lambda_{\text{ex}} = 490 \text{ nm}$) upon the addition of various amounts of NPY-1 (a), NPY-2 (b) and NPY-3 (c) in a HEPES (10 mM, pH = 7.4) buffered solution. The inset shows the fluorescence intensity of UD at 515 nm versus the equiv of NPY-1, NPY-2 and NPY-3.

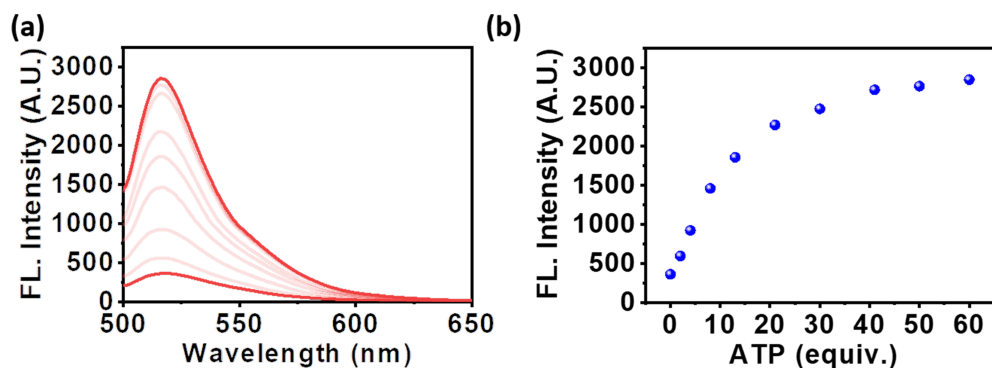


Fig. S11 (a) Fluorescence spectra of NPY-1/UD (66 $\mu\text{M}/6 \mu\text{M}$, $\lambda_{\text{ex}} = 490 \text{ nm}$) upon the addition of various amounts of ATP in a HEPES (10 mM, pH = 7.4) buffered solution. (b) Fluorescence intensity of NPY-1/UD at 515 nm versus the number of equiv of ATP.

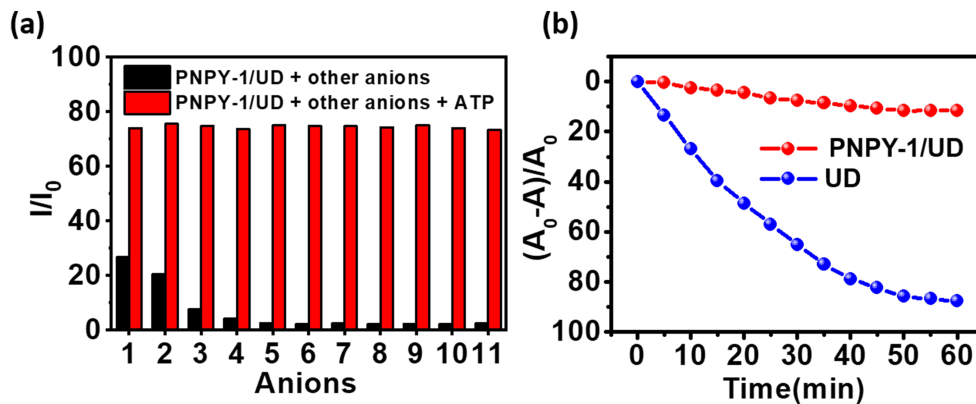


Fig. S12 (a) Competitive fluorescence experiment of probe **PNPY-1/UD** toward ATP in the presence of various anions in HEPES (10 mM, pH = 7.4) buffer solutions. 1-ADP, 2-PPi, 3-AMP, 4- H_2PO_4^- , 5- AcO^- , 6- F^- , 7- Cl^- , 8- Br^- , 9- I^- , 10- CO_3^{2-} , 11- SO_4^{2-} . (b) The relative absorption loss (%) of UD (6 μM , record at 490 nm) and PNPY-1/UD (12 $\mu\text{M}/6 \mu\text{M}$, record at 517 nm) with exposure time at xenon lamp (300 W) irradiation.

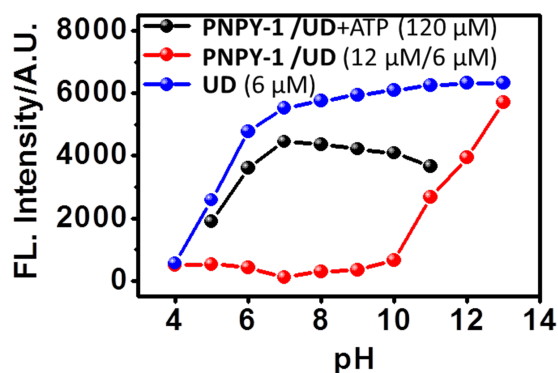


Fig. S13 Fluorescence intensity at 515 nm of UD (6 μM), PNPY-1/UD (12 $\mu\text{M}/6 \mu\text{M}$) and PNPY-1/UD + ATP (10 equivalents) at different pH values.

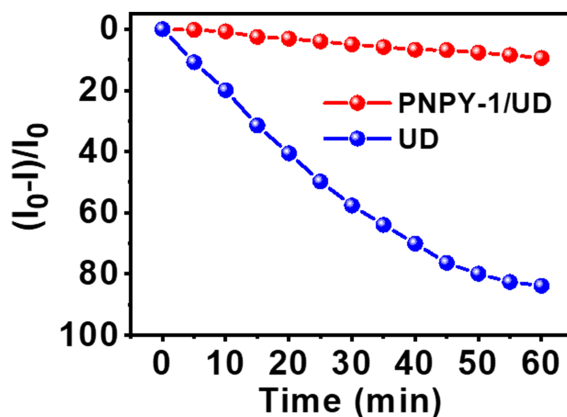


Fig. S14 The relative fluorescence loss of UD (12 $\mu\text{M}/6 \mu\text{M}$) and PNPY-1/UD (12 $\mu\text{M}/6 \mu\text{M}$) with increasing the exposure time of xenon lamp (300 W) at 517 nm.

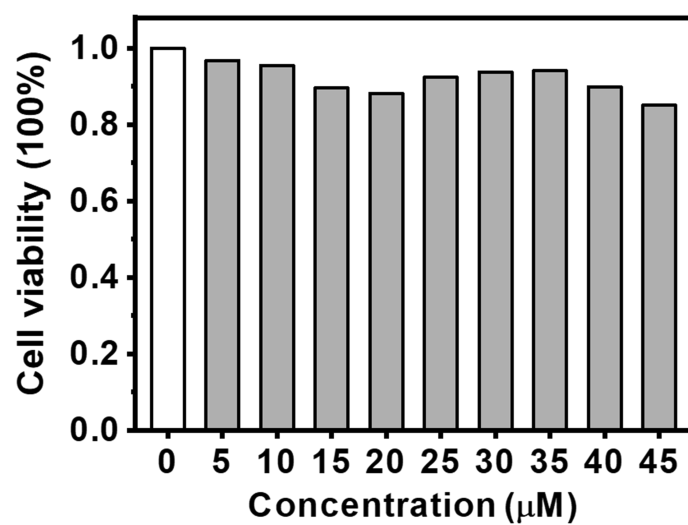


Fig. S15 Cell viability after incubation of Hepa1-6 murine liver cancer cells with various concentrations of **PNPY-1/UD** in aqueous solutions.

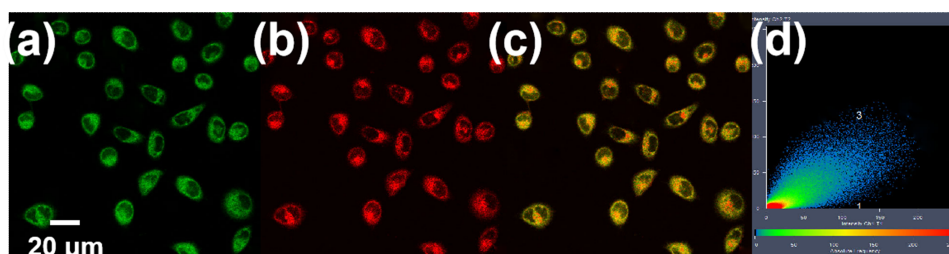


Fig. S16 Laser scanning confocal images of Hepa1-6 cells co-stained with **PNPY-1/UD** (12 μM/6 μM) and CytoFixRed (10 μM) for 30 min. (a) Ex. 488 nm, Em. 500–570 nm, (b) Ex. 488 nm, Em. 650–710 nm. (c) Merged image of (a) and (b). Scale bar, 20 μm. (d) Correlation plot of **PNPY-1/UD** and CytoFixRed intensities (Pearson Correlation Coefficient: 0.82).

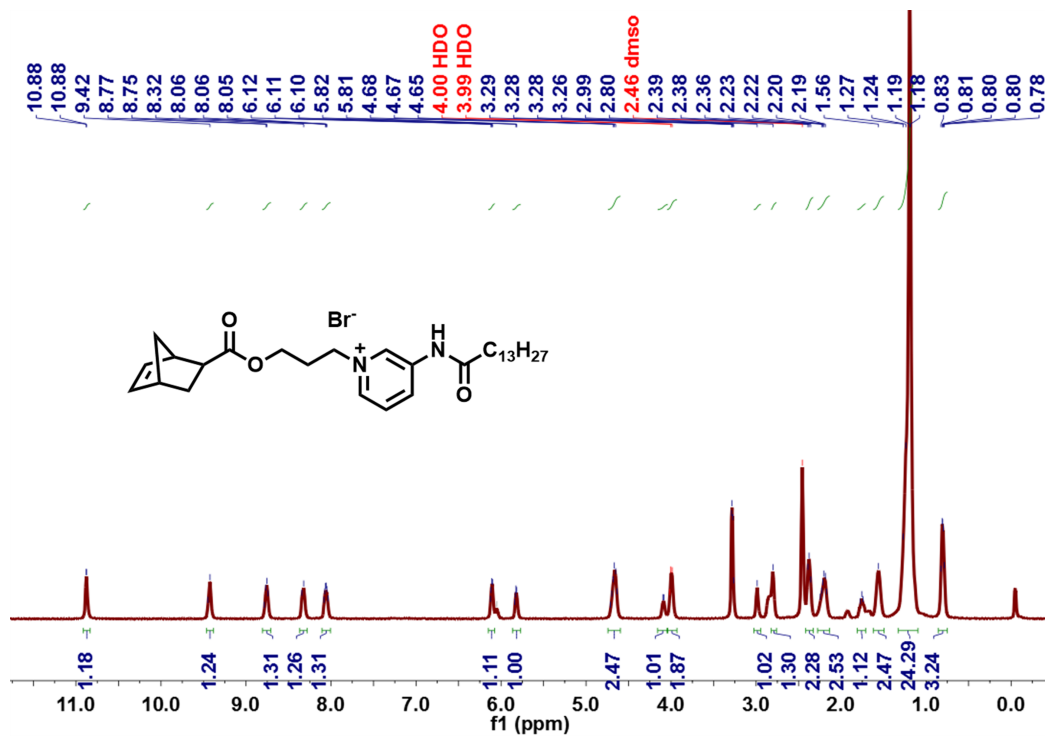


Fig. S17 ^1H NMR spectrum of NPY-1 in a $\text{DMSO-}d_6$ solution.

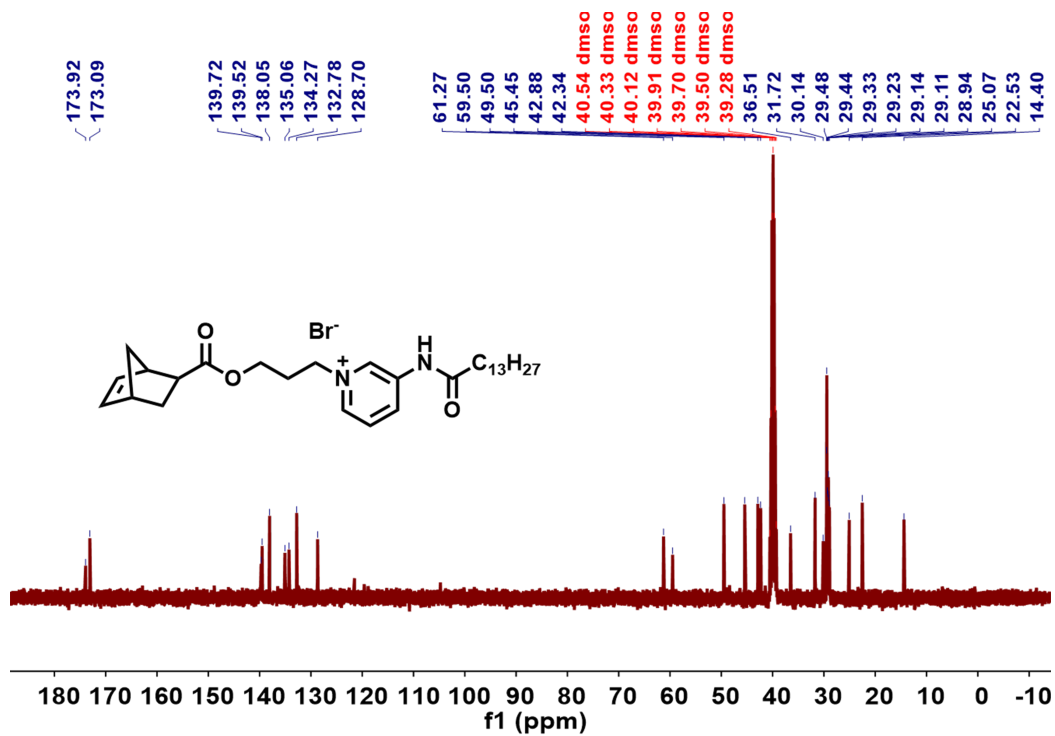


Fig. S18 ^{13}C NMR spectrum of NPY-1 in a $\text{DMSO-}d_6$ solution.

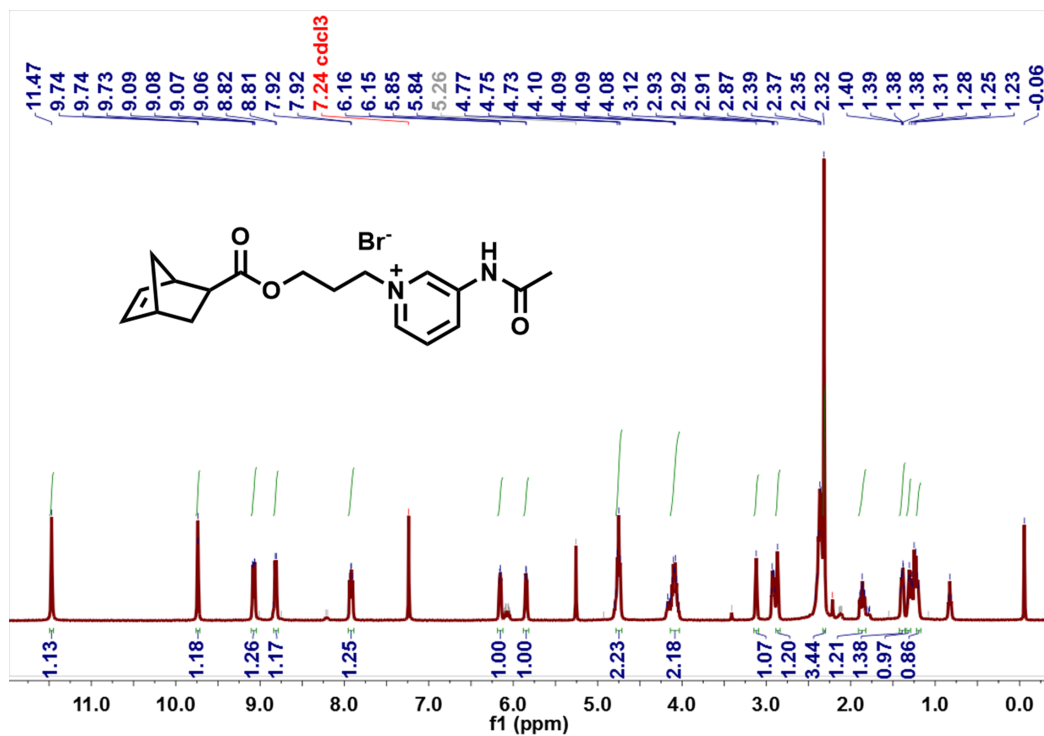


Fig. S19 ^1H NMR spectrum of NPY-2 in a $\text{DMSO-}d_6$ solution.

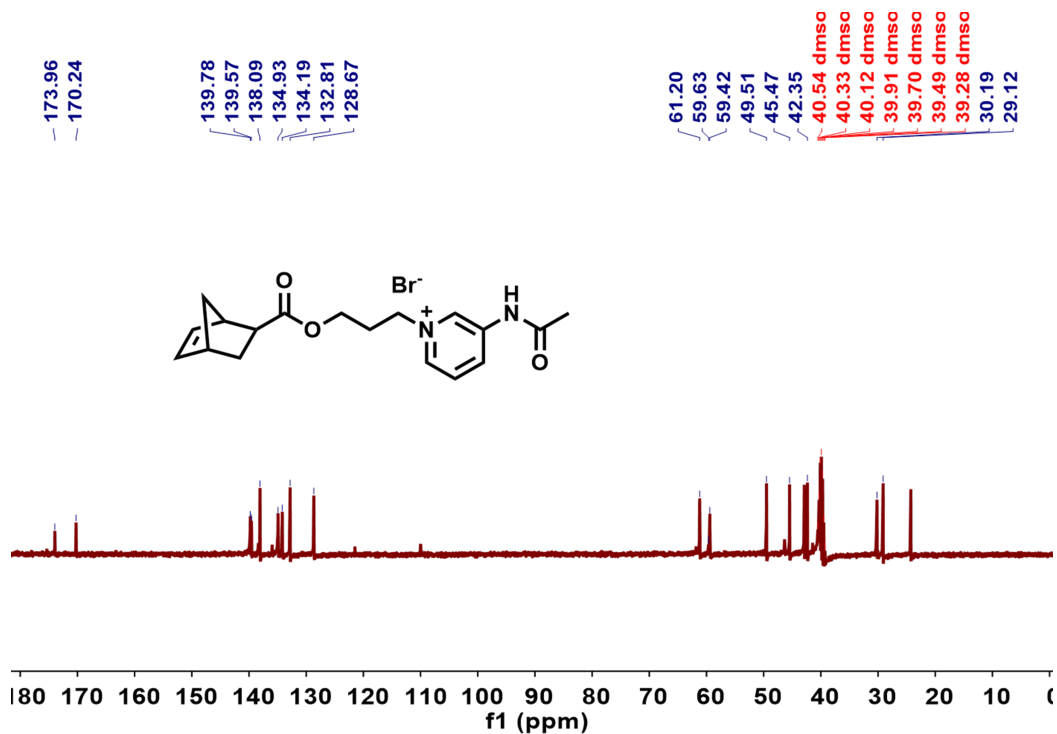


Fig. S20 ^{13}C NMR spectrum of NPY-2 in a $\text{DMSO-}d_6$ solution.

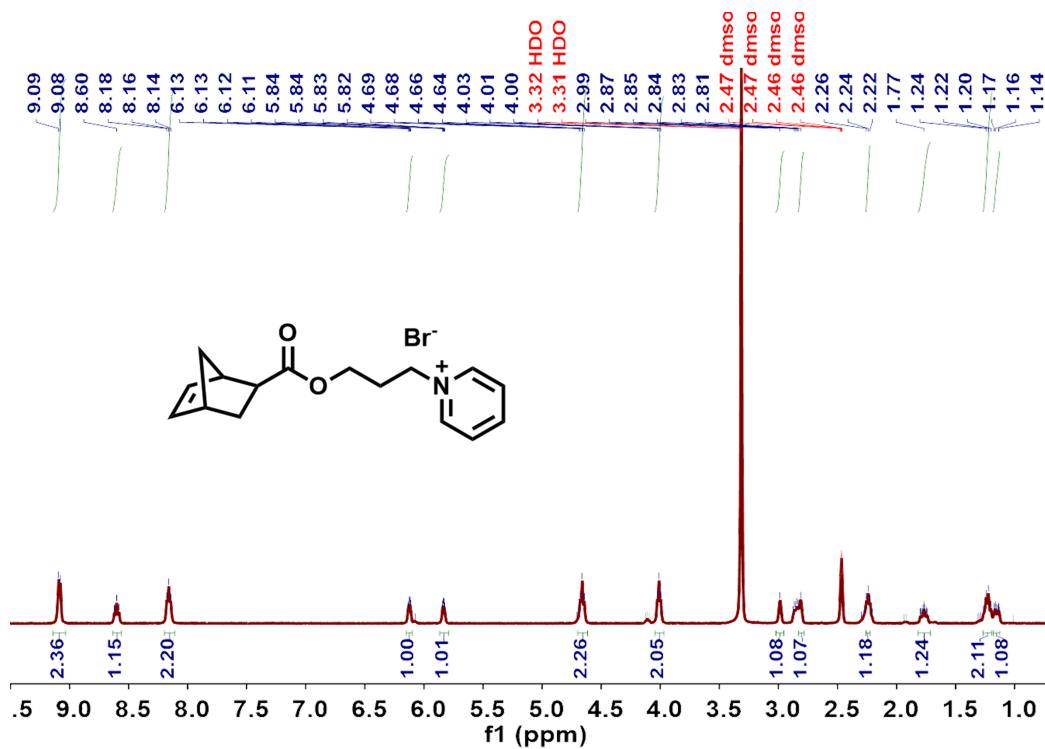


Fig. S21 ^1H NMR spectrum of NPY-3 in a $\text{DMSO-}d_6$ solution.

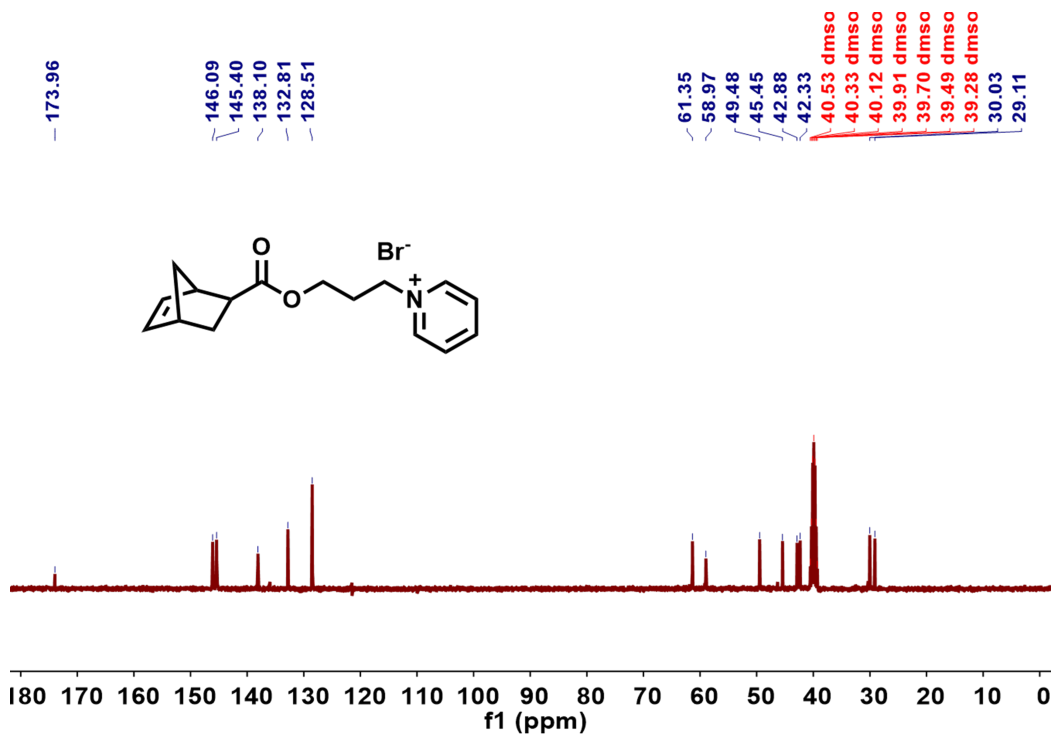


Fig. S22 ^{13}C NMR spectrum of NPY-3 in a $\text{DMSO-}d_6$ solution.

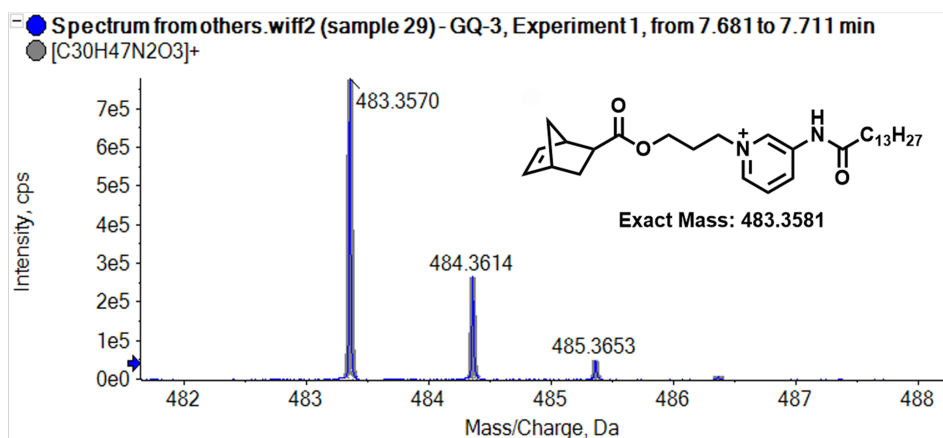


Fig. S23 The HR-MS spectrum of NPY-1

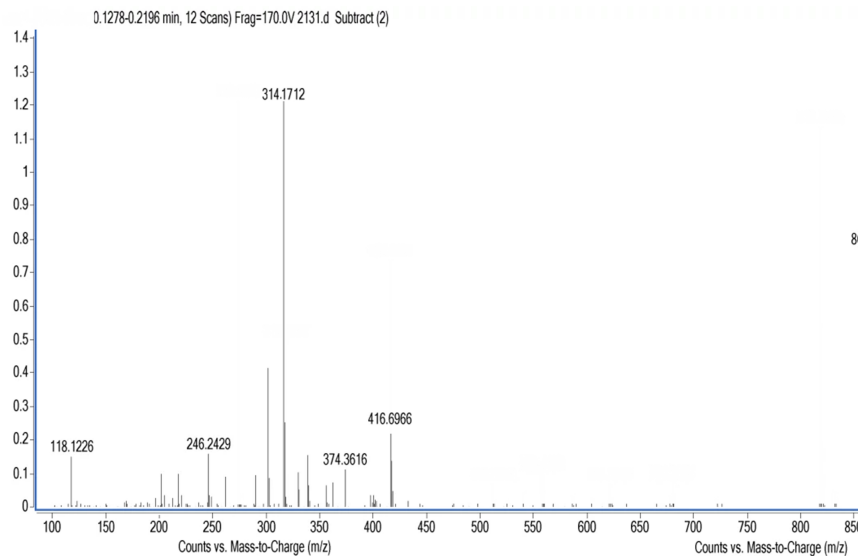


Fig. S24 The HR-MS spectrum of NPY-2

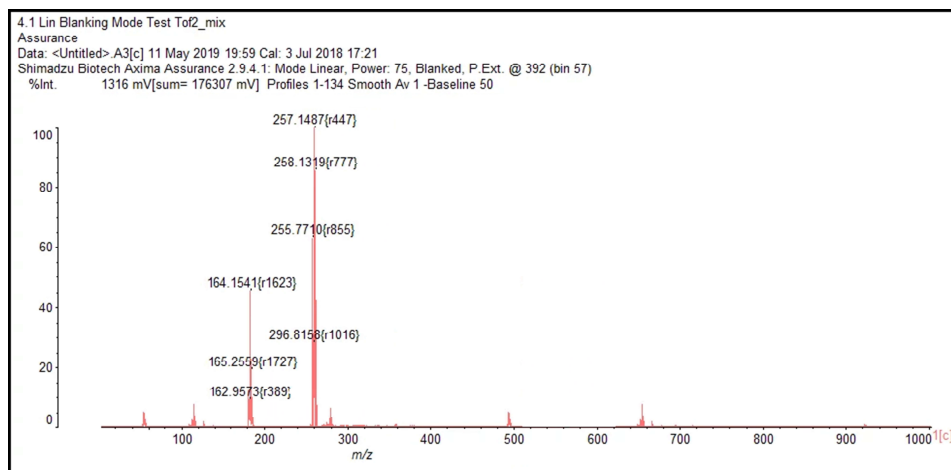


Fig. S25 The HR-MS spectrum of NPY-3

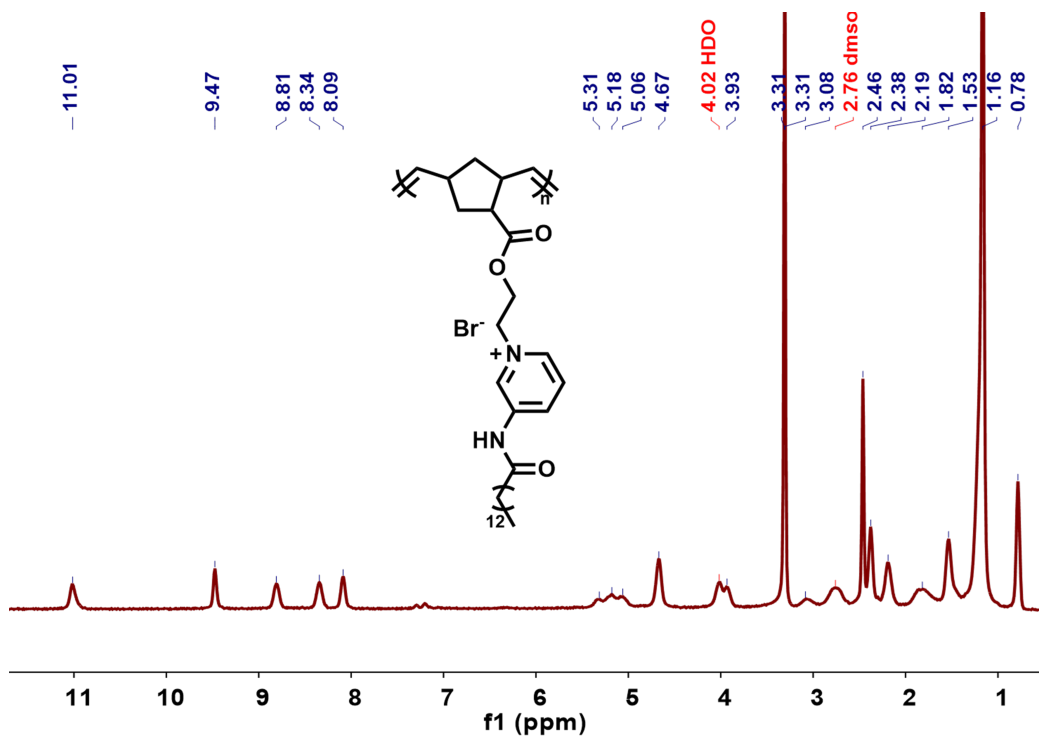


Fig. S26 ^1H NMR spectrum of PNPY-1 in a $\text{DMSO-}d_6$ solution.

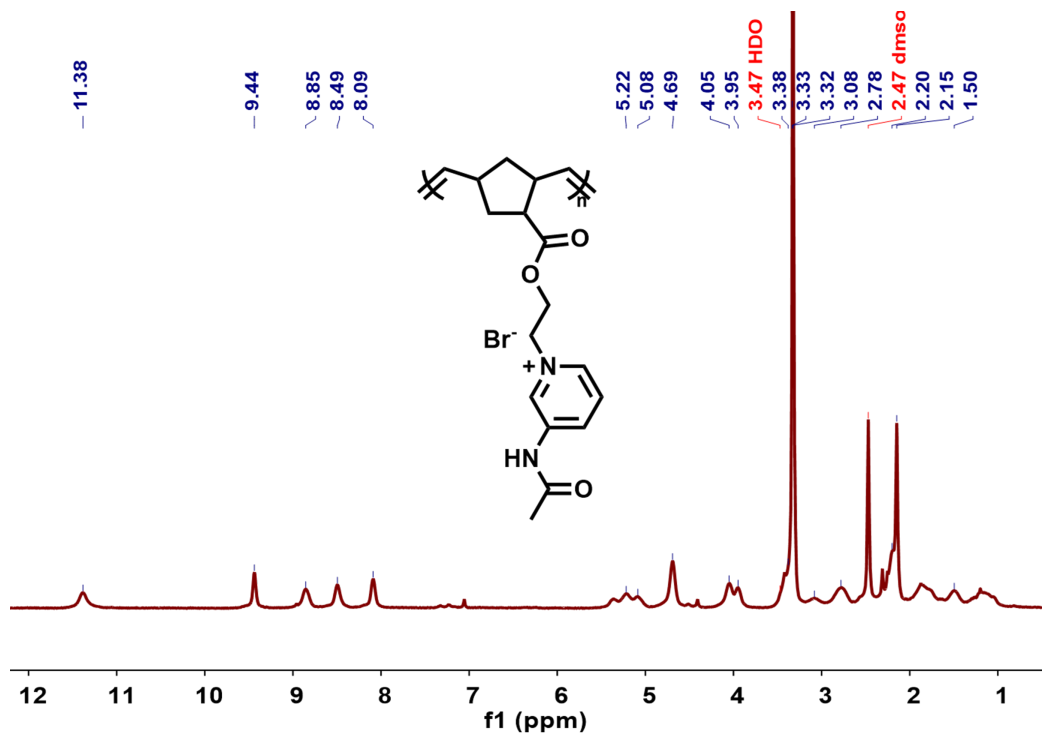


Fig. S27 ¹H NMR spectrum of PNPY-2 in a DMSO-*d*₆ solution.

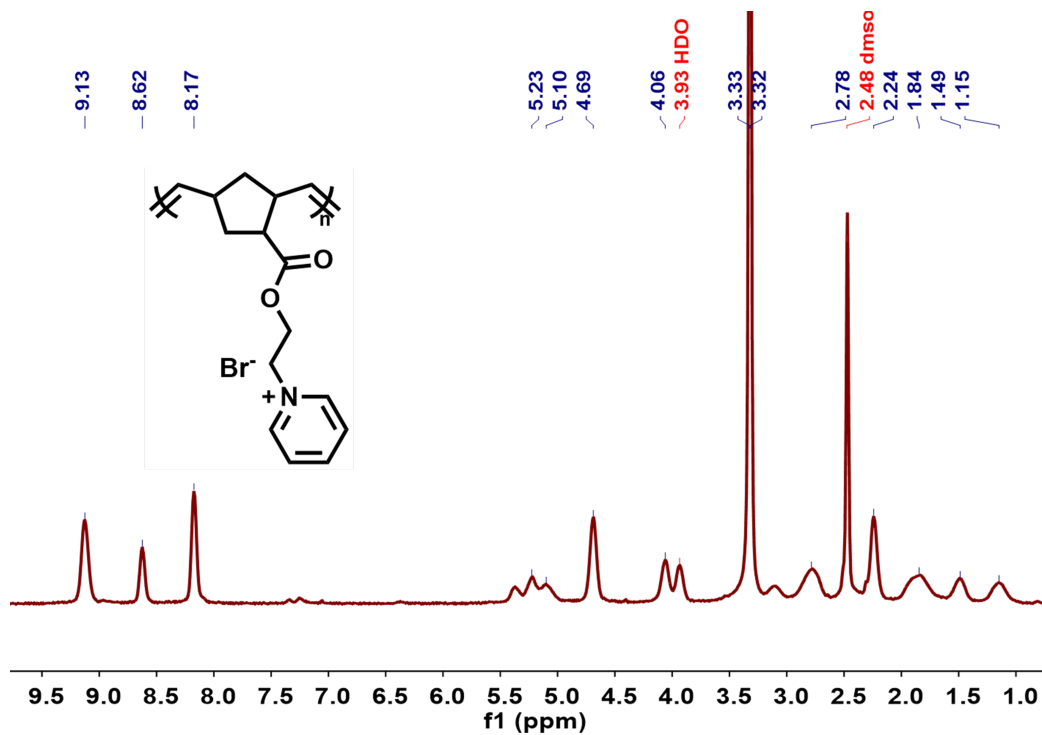


Fig. S28 ¹H NMR spectrum of PNPY-3 in a DMSO-*d*₆ solution.

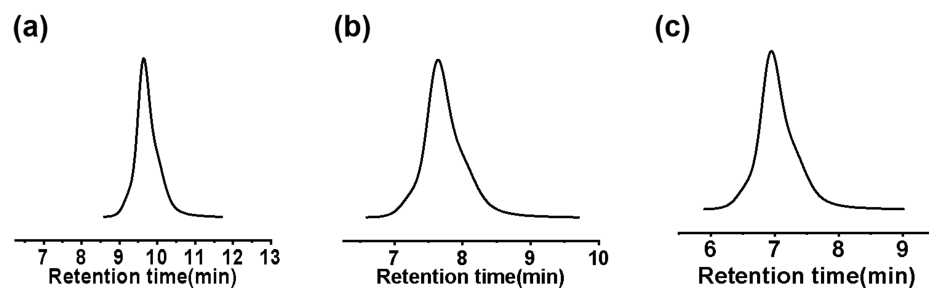


Fig. S29 The GPC curve of (a) PNPY-1; (b) PNPY-2; (c) PNPY-3 in THF, polystyrene standard.

References

- [1] S. Brahmachari, S. Debnath, S. Dutta, P. K. Das, *Beilstein J. Org. Chem.*, 2010, **6**, 859–868.
- [2] S. K. Yang, M. Weck, *Macromolecules*, 2008, **41**, 346–351.